

Sublattice model of atomic scale pairing inhomogeneity in a superconductor

Vivek Mishra* and P. J. Hirschfeld†

Department of Physics, University of Florida, Gainesville, Florida 32611-8440, USA

Yu. S. Barash

Institute of Solid State Physics, Russian Academy of Sciences, Chernogolovka, 142432 Russia

(Dated: May 29, 2019)

We study a toy model for a superconductor on a bipartite lattice, where intrinsic pairing inhomogeneity is produced by two different coupling constants on the sublattices. The simplicity of the model allows for analytic solutions and tests of the consequences of atomic-scale variations in pairing interactions which have been considered recently in the cuprates. We present results for the transition temperature, density of states, and thermodynamics of the system over a phase diagram in the plane of two pairing coupling constants. For coupling constants of alternating sign, a gapless superconducting state is stable. Inhomogeneity is generally found to enhance the critical temperature, and at the same time the superfluid density is remarkably robust: at $T = 0$, it is suppressed only in the gapless phase.

PACS numbers: 74.81.-g, 74.62.-c, 74.78.Na, 74.25.Dw

I. INTRODUCTION

In recent years, the effect of underlying inhomogeneities in superconductors has attracted many researchers. In the context of high temperature superconductors (HTSC), checkerboard local density of states (LDOS) oscillations and strong nanoscale gap inhomogeneity have been observed in scanning tunnelling spectroscopy (STS) experiments¹, and signals in dynamical susceptibility measured by neutron scattering have been interpreted as stripelike nanoscale modulations of charge and spin degrees of freedom². While it is still not clear whether these modulations are intrinsic in nature or driven entirely by disorder, others have pointed out that the very existence of inhomogeneity may enhance T_c , and implicitly suggested that the phenomenon of high critical temperatures may rely on it^{3,4}. In particular, Martin et al.³ studied a simple model, in which they included a 1D inhomogeneous pair potential varying on an arbitrary length scale $\ell \gtrsim a$, where a is the lattice spacing, and argued for an increase of the critical temperature with inhomogeneity, with a maximum enhancement obtained for $\ell \simeq \xi_0$, where ξ_0 is the coherence length of the analog homogeneous system. Similar results were obtained by Loh and Carlson, where they found however that an increase in the transition temperature occurred at the cost of reduced superfluid density⁵. Aryanpour et al.⁶ performed a systematic numerical study of s -wave superconductivity on checkerboard, stripe and random patterns of pairing potentials in an attractive Hubbard model; they also found a positive correlation between critical temperature and inhomogeneity for many situations. It is also known that models with enhanced T_c and significant inhomogeneity are associated with unusual features in electronic structure. For example, recent calculations of high-quality ultrathin s -wave superconducting films have shown that the surface-driven inhomogeneity can enhance T_c due to weakly dispersive low-energy subgap

states in the system⁷. The above studies were primarily considerations of BCS type models. Recently, however, Tsai et al.⁸ have studied small size repulsive Hubbard models with a “checkerboard”-like modulation of hopping matrix elements using exact diagonalization, and also concluded that the inhomogeneous models could lead to pairing at very high binding energy scales.

Nunner et al.⁹ underlined the importance of this phenomenon for cuprates by explaining many of the correlations between the measured local gap and other observables in Bi-2212 by assuming a d -wave pairing interaction $g(\mathbf{r})$ varying on a unit cell size, and driven by dopant disorder. If the effective pair interaction can vary on an atomic scale, and the BCS coherence length is sufficiently short, one can imagine situations where in a complex periodic crystal with large unit cell the pairing interaction varies over an atomic length scale in the absence of disorder, i.e. a periodic, modulated $g(\mathbf{r})$, which will give rise to a periodic, modulated order parameter $\Delta(\mathbf{r})$. The properties of such a system are important to understand, because it represents the simplest type of nanoscale pairing modulation, and one may study the relationship between superconducting properties and inhomogeneity easily. Aryanpour et al.⁶ considered systems of this type within a purely numerical approach, and obtained a variety of interesting results. Nevertheless, in such a treatment it is sometimes difficult to extract simple conclusions and understand exactly which aspects of superconductivity are really enhanced or suppressed by inhomogeneity, and why.

In this paper, we consider the simplest such model, a bipartite lattice in two dimensions with two different values of g on two interpenetrating sublattices. The homogeneous version of the model has a superconducting ground state on a bipartite lattice in arbitrary dimension and filling¹⁰. Here we calculate the ground state and thermodynamics of this system for any values (g_A, g_B) , where A and B represent the two sublattices. We distin-

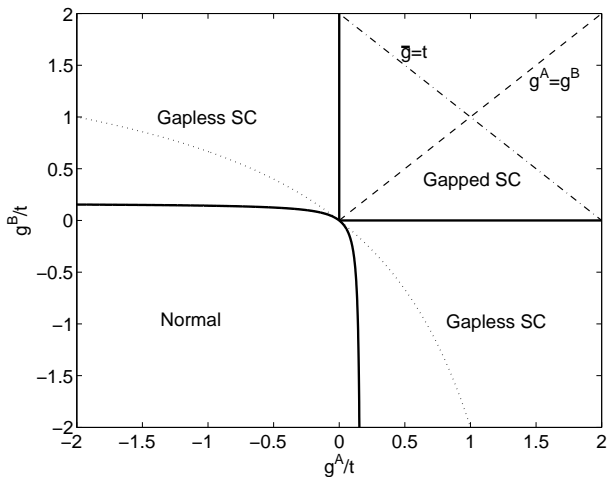


FIG. 1: $T = 0$ mean field phase diagram in the space of two coupling constants g_A and g_B found in this paper. The solid lines represent transitions between normal metal (defined by $\Delta_A = \Delta_B = 0$), gapped and gapless superconducting phases. The dashed-dotted line represents the line of constant average pairing $\bar{g} = t$ studied in the text. The dashed line represents the homogeneous BCS case with $g^A = g^B$. Finally, the dotted line represents the normal-gapless superconducting transition line as calculated analytically within the approximation described in the text using the “window” density of states (wDOS).

guish however two cases: one, where both g 's have the same sign; and a second, where they differ. Situations like the latter case where the pairing potential changes sign abruptly over a unit cell distance have been considered in the impurity context^{11,12}, but not in periodic cases, and it is not clear whether true superconducting solutions can exist in such a situation.

In section II, we introduce the sublattice pairing model and give exact expressions for the order parameter and critical temperature T_c within the generalized BCS scheme. We show that T_c can indeed be enhanced by detuning the coupling constants from the BCS point $g_A = g_B$. We then derive in section III the quasiparticle excitations and thermodynamic properties of the model. When the average pairing strength is held constant but inhomogeneity is increased, the model displays a shrinking spectral gap in the total DOS. In the case of opposite sign coupling constants, the excitation spectrum becomes gapless, and the mean field solution corresponds to an order parameter which oscillates in sign from point to point. In section IV, we calculate the superfluid density n_s for the model, and show that for the case of same-sign coupling constants inhomogeneity preserves a robust n_s at $T = 0$. In the case of opposite signs, however, n_s is suppressed by the onset of a residual normal fluid. The variations of superconducting phenomenology found in our solution to the model is summarized in the phase diagram shown in Fig. 1.

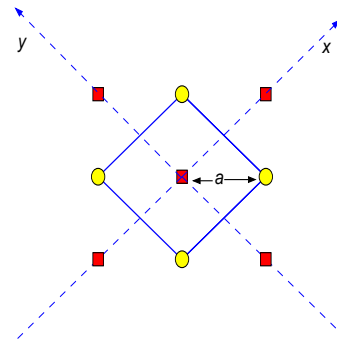


FIG. 2: Unit cell of square lattice, where squares and circles denote sites of type “A” and “B”, and the lattice spacing is denoted by a , which we have set to 1 throughout our discussion. The coordinate system used in Fourier transformation is shown with two dashed lines.

II. MODEL

The Hamiltonian is given by Eq. (1), where c_i, c_i^\dagger are the electron annihilation and creation operators. t is the strength of hopping energy between the nearest neighbors and Δ_i is the mean field gap at site i . The sum in the Hamiltonian is over all sites and spins denoted by σ . The unit cell of the bipartite lattice is shown in Fig. 2, and the Fourier transformation in Eq. (2) is defined with respect to this cell. We first consider the case of half-filling, for which the chemical potential μ is set to zero.

$$H = \sum_{i,\delta,\sigma} -tc_{i,\sigma}^\dagger c_{i+\delta,\sigma} + \Delta_i c_{i,\sigma}^\dagger c_{i,-\sigma}^\dagger. \quad (1)$$

In anticipation of the doubling of the unit cell due to an interaction specified on each sublattice, we Fourier transform fermionic operators as

$$c_{i,\sigma} = \sum_{\mathbf{k}} c_{\mathbf{k},\sigma} e^{i\mathbf{k}\cdot\mathbf{r}_i}, \quad (2)$$

where the sum now runs over the arising for staggered ordering (“antiferromagnetic”) half-Brillouin zone specified by $0 \leq |k_i| \leq \pi/(\sqrt{2}a)$ for $i = x, y$, with directions specified in Fig. 2. The Hamiltonian now becomes

$$\begin{aligned} H &= \sum_{\mathbf{k},\sigma} \xi_{\mathbf{k}} c_{\mathbf{k}\sigma}^{\dagger A} c_{\mathbf{k}\sigma}^B + \Delta^A c_{\mathbf{k}\sigma}^{\dagger A} c_{\mathbf{k}-\sigma}^{\dagger A} + \Delta^B c_{\mathbf{k}\sigma}^{\dagger B} c_{\mathbf{k}-\sigma}^B \quad (3) \\ &= \sum_{\mathbf{k}} \tilde{c}_{\mathbf{k}}^\dagger \cdot M \cdot \tilde{c}_{\mathbf{k}}, \quad (4) \end{aligned}$$

where we have assumed s -wave pairing and the dispersion relation is given by

$$\xi_{\mathbf{k}} = -4t \cos\left(\frac{k_x}{\sqrt{2}}\right) \cos\left(\frac{k_y}{\sqrt{2}}\right). \quad (5)$$

The matrix M may be expressed as

$$M = \begin{bmatrix} 0 & \xi_k & \Delta^A & 0 \\ \xi_k & 0 & 0 & \Delta^B \\ \Delta^A & 0 & 0 & -\xi_k \\ 0 & \Delta^B & -\xi_k & 0 \end{bmatrix} \quad (6)$$

in the staggered particle-hole space spanned by $\tilde{c}_{\mathbf{k}} = (c_{-\mathbf{k}\sigma}^A, c_{-\mathbf{k}\sigma}^B, c_{\mathbf{k}-\sigma}^{A\dagger}, c_{\mathbf{k}-\sigma}^{B\dagger})$. After performing the canonical transformation

$$c_{\mathbf{k}\sigma}^{\dagger\alpha} = u_n^{*\alpha}(\mathbf{k})\gamma_{\mathbf{k}\sigma}^{\dagger} + \sigma v_n^{\alpha}(\mathbf{k})\gamma_{\mathbf{k},-\sigma}, \quad (7)$$

with $\alpha = A, B$, we find the quasiparticle energies $\pm E_{1,2}$, with

$$E_{1,2} = \frac{\mp \Delta^A \pm \Delta^B + \sqrt{(\Delta^A + \Delta^B)^2 + 4\xi_{\mathbf{k}}^2}}{2}, \quad (8)$$

which reduce to the usual $E_{\mathbf{k}} = \sqrt{\xi_{\mathbf{k}}^2 + \Delta^2}$ for $\Delta^{\alpha} \rightarrow \Delta$.

The eigenstates of the problem, of the form $|u_A, u_B, v_A, v_B\rangle$, are given by

$$|\lambda_1, -E_1\rangle = [-x_1, -x_2, -x_1, x_2] \frac{1}{\sqrt{2(x_1^2 + x_2^2)}}, \quad (9)$$

$$|\lambda_2, -E_2\rangle = [-x_2, -x_1, x_2, -x_1] \frac{1}{\sqrt{2(x_1^2 + x_2^2)}}, \quad (10)$$

$$|\lambda_3, E_2\rangle = [-x_2, x_1, -x_2, -x_1] \frac{1}{\sqrt{2(x_1^2 + x_2^2)}}, \quad (11)$$

$$|\lambda_4, E_1\rangle = [-x_1, x_2, x_1, x_2] \frac{1}{\sqrt{2(x_1^2 + x_2^2)}}, \quad (12)$$

where

$$x_{1,2} = \sqrt{\sqrt{(\Delta^A + \Delta^B)^2 + 4\xi^2} \mp (\Delta^A + \Delta^B)}. \quad (13)$$

Using the definition of the gap functions,

$$\Delta_{\bar{k}}^{\alpha} = g^{\alpha} \langle c_{\bar{k}\sigma}^{\alpha} c_{\bar{k}-\sigma}^{\alpha} \rangle = \sum_n u_{n,\alpha} v_{n,\alpha}^* \text{th} \left(\frac{\beta E_n}{2} \right) \quad (14)$$

we can write down the gap equation for the Δ^{α}

$$\begin{aligned} \Delta^A &= \sum_{\bar{k}} \frac{g^A}{x_1^2 + x_2^2} \left\{ -x_1^2 \text{th} \left(\frac{\beta E_1}{2} \right) + x_2^2 \text{th} \left(\frac{\beta E_2}{2} \right) \right\}, \\ \Delta^B &= \sum_{\bar{k}} \frac{g^B}{x_1^2 + x_2^2} \left\{ x_2^2 \text{th} \left(\frac{\beta E_1}{2} \right) - x_1^2 \text{th} \left(\frac{\beta E_2}{2} \right) \right\}. \end{aligned} \quad (15)$$

Note that within our convention a positive g corresponds to an attractive on-site interaction. We now calculate T_c by linearizing the gap equations. To obtain analytical results, we estimate the integrals involved using the approximate window density of states (wDOS)

$$\rho(\omega) = \begin{cases} 1/8t & -4t \leq \omega \leq 4t \\ 0 & \text{elsewhere} \end{cases}, \quad (16)$$

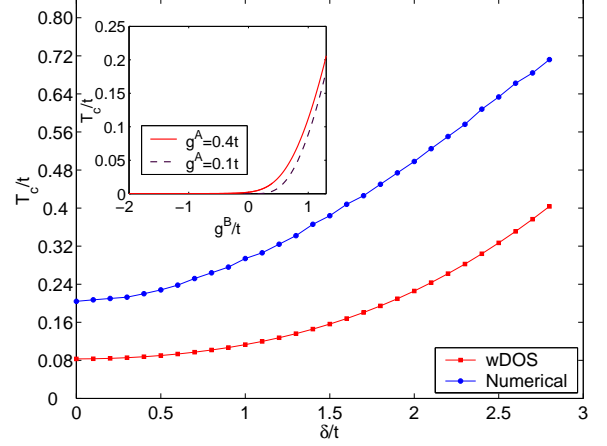


FIG. 3: Critical temperature T_c/t plotted vs. difference of sublattice coupling constants $\delta \equiv (g^A - g^B)/t$ for fixed $\bar{g} = t$. Squares: window density of states. Circles: exact. Insert: $T_c/(4t)$ vs. g^B/t for fixed $g^A = t$.

which is a good approximation for the tight binding model for qualitative purposes. Then T_c takes the form

$$\begin{aligned} k_B T_c &\simeq \left(\frac{8te^\gamma}{\pi} \right) \exp \left(-\frac{1}{\bar{g}_{eff}} \right), \\ \bar{g}_{eff} &\equiv \frac{4g^A g^B - 8t(g^A + g^B)}{8t(g^A + g^B) - (8t)^2}. \end{aligned} \quad (17)$$

The dimensionless effective interaction \bar{g}_{eff} plays the same role as the single attractive coupling constant in BCS weak-coupling theory. The phase transition to the normal state takes place as $\bar{g}_{eff} \rightarrow 0^+$, determining the dotted line in Fig. 1. Note that the mathematical expression for T_c (17) actually diverges as $\bar{g}_{eff} \rightarrow 0^-$, i.e. as one approaches the phase transition from the normal state side, again in perfect analogy with BCS. The apparent nonzero value for T_c on this side is of course spurious, as there is no ordering below this temperature, as will be shown below.

This estimate for T_c is compared in Figs. 1 and 3 with the exact numerical solution for the normal state instability temperature from Eqs. 15. In order to judge the extent to which inhomogeneity enhances superconductivity, in this work we keep the average pairing interaction per site, $\bar{g} \equiv (g^A + g^B)/2$, fixed unless otherwise stated, and plot T_c vs. the difference $\delta \equiv (g^A - g^B)$. We see that the numerical discrepancies between the exact evaluation and the window DOS approximation are in fact quite large, due to the presence of the van Hove singularity at the Fermi level in the simple 2D band, together with the exponential dependence of T_c on the density of states, but that the approximation captures the qualitative dependence of T_c on inhomogeneity. It is clear that, as in other mean field models of inhomogeneous

pairing, the inhomogeneity enhances the critical temperature. We return in Sec. IV to the question of when this result breaks down.

If, instead of holding the average interaction \bar{g} fixed, we fix the attractive interaction on one sublattice g^A and progressively decrease g^B , we find a rapidly decreasing T_c (see insert to Fig. 3). Depending on the magnitude of g^B , we either see only an exponential decrease of T_c or, for very small g^B , an instability to the metallic state at a critical value determined by the change of sign of the effective interaction. This determines the solid line in the phase boundary corresponding to the transition to the normal state shown in Fig. 1.

III. QUASIPARTICLE STATES AND THERMODYNAMICS

A. Order parameters

We now consider the order parameters Δ^α which develop below T_c on the two sublattices. It turns out that there are two different cases, which we discuss separately, corresponding to coupling constants on the two sublattices of identical or opposite sign. In general, we can write using Eqs. (15),

$$\frac{\Delta^A}{g^A} - \frac{\Delta^B}{g^B} = \sum_{\vec{k}} \left[\tanh\left(\frac{\beta E_2}{2}\right) - \tanh\left(\frac{\beta E_1}{2}\right) \right] \quad (18)$$

We first assume both coupling constants positive, $0 \leq g_B \leq g_A$. If both gaps are positive, then E_1, E_2 are positive. Therefore in limit $T \rightarrow 0$ the right hand side of Eq. (18) will vanish, which gives the solution:

$$\frac{\Delta^A}{\Delta^B} = \frac{g^A}{g^B}, \quad (19)$$

which is exact for the case of both g 's attractive. Now if we employ the window density of states given by Eq. (16), we obtain

$$\Delta^\alpha \simeq \frac{g^\alpha}{g^A + g^B} \frac{8t}{\sinh\left(\frac{8t}{g^A + g^B}\right)} \quad (20)$$

For $g^A = g^B$, within weak coupling approximation ($g^{A,B} \ll 8t$), this gives $\Delta/k_B T_c = e^\gamma/\pi$, which is the standard BCS result.

The exact solution for the temperature dependence of the gap is shown for the case of weak inhomogeneity in Fig. 4(a).

Now we consider the other case when one of the coupling constants is negative, $g_B \leq 0 < g_A$. From (15) we see that Δ^B is forced to be negative. The variation of gap as a function of temperature found numerically

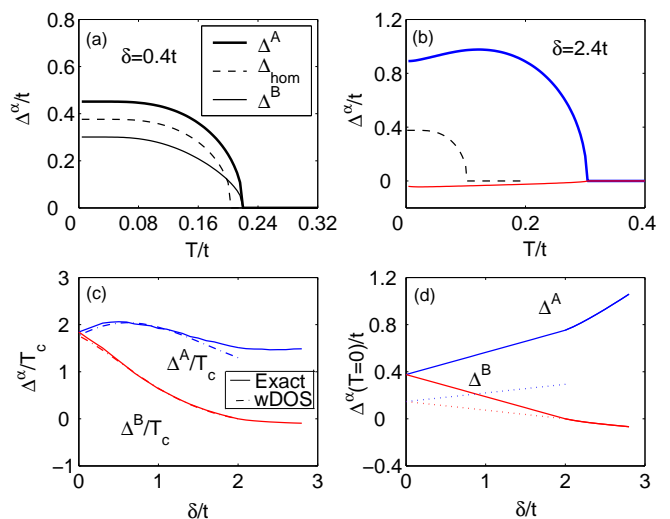


FIG. 4: (a) Sublattice order parameters $\Delta^{A,B}$ vs. T/t for weak inhomogeneous pairing interaction $\delta \equiv (g^A - g^B) = 0.4t$; (b) strong inhomogeneous cases, with $\delta = 2.4t$ (note $g^B = -0.2t$). (c) Ratio $\Delta^\alpha(T=0)/T_c$ vs. δ for $\alpha = A, B$ (solid line: full numerical evaluation; dashed-dotted line: wDOS); (d) Comparison of full numerical evaluation of $\Delta^\alpha(T=0)$ (solid line) with wDOS approximation (dashed-dotted line). For all plots, the average coupling is fixed to $\bar{g} = 1$. Note in (c),(d) that the gapless phase discussed in Sections III B and III C correspond, for the parameters given here, to $2 \leq \delta/t$.

and displayed in Fig. 4(b) is somewhat unusual. As the temperature increases from zero, the gap increases in magnitude and then after attaining a maximum value begin to decrease.

In the case of opposite sign coupling constants, relation (19) is no longer valid. In this case one can obtain an approximate analytical expression for $|\Delta^B|/\Delta^A$ using the wDOS (16), but it is quantitatively inaccurate. A more accurate approximation is obtained by replacing the exact contour of zero quasiparticle energy with a square of side $2\sqrt{2} \cos^{-1}\left(\frac{\sqrt{|\Delta^A|\Delta^B|}}{4t}\right)$. This turns out to be equivalent to a renormalized wDOS approximation where the bare bandwidth $8t$ is replaced by $4\pi t$. We find

$$\frac{|\Delta^B|}{\Delta^A} = \left(\frac{g^B}{2\pi t}\right)^2 \left(\sqrt{\frac{4\pi^2 t^2}{g^A |g^B|} + 1} - 1\right)^2. \quad (21)$$

In Figs. 4 (c) and (d) we illustrate the utility of the wDOS and renormalized wDOS approximations with which analytical results were obtained above. While Fig. 4(d) shows that the inaccuracies arising from the wDOS also influence the value of the $T=0$ order parameters on the two sublattices, the qualitative tendencies with δ are well reproduced. Furthermore, the ratios $\Delta^{A,B}/T_c$ agree quantitatively with the exact numerical results over a wide range of inhomogeneities (Fig. 4(c)), as the errors introduced in the DOS are largely cancelled by taking

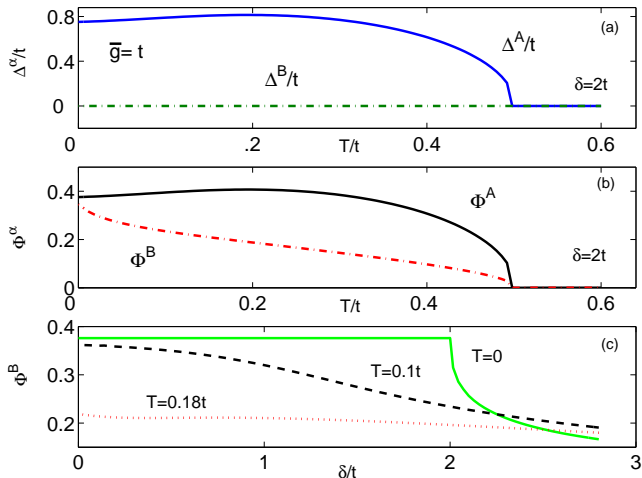


FIG. 5: (a) Gaps $\Delta^{A,B}/(4t)$ vs. $T/(4t)$ for special case $\delta = 2t$, $\bar{g}=t$ ($g^B = 0$); (b) Condensate amplitude $\Phi^B \equiv \langle c^B c^B \rangle$ for same case as (a); (c) Variation of Φ^B with inhomogeneity δ/t for three different temperatures $T/t = 0, 0.11, 0.18t$.

the ratio.

The normal state region shown in the phase diagram of Fig. 1 represents the metallic phase where, within the current mean field treatment, the only solution found has both order parameters $\Delta^{A,B} = 0$.

B. Condensate amplitudes

There are several measures of the “strength of superconductivity” in a material which become distinct when the material is inhomogeneous. One is the order parameter, which we have discussed above. A second is the pair wave function, or condensate amplitude $\Phi^\alpha \equiv \langle c_{-\mathbf{k}-\sigma}^\alpha c_{\mathbf{k}\sigma}^\alpha \rangle$, such that $\Delta^\alpha = g^\alpha \Phi^\alpha$. To illustrate the differences, it is useful to consider first an interesting if artificial special case where the coupling is attractive on one sublattice and vanishes on another. We therefore take $g^A = 2t$ and $g^B = 0$, and plot both the order parameters and condensate amplitudes in Fig. 5.

Using the wDOS, the condensate on either the A or B sublattice for the $g^B = 0$ case can be obtained analytically at $T = 0$ as

$$\Phi^\alpha = 4 \sinh^{-1} \left[\frac{1}{2 \sinh(8t/g^A)} \right] \quad (\alpha = A, B, \quad g_B = 0) \quad (22)$$

In other words, although the pairing interaction on the B sublattice is zero, the proximity effect is so strong that a uniform condensate fraction is induced over the entire system. This degeneracy is broken at finite temperatures, where the B condensate is weakened relative to that on the A sublattice. Of course, the order parameter on the B sublattice is zero at all temperatures due to the ab-

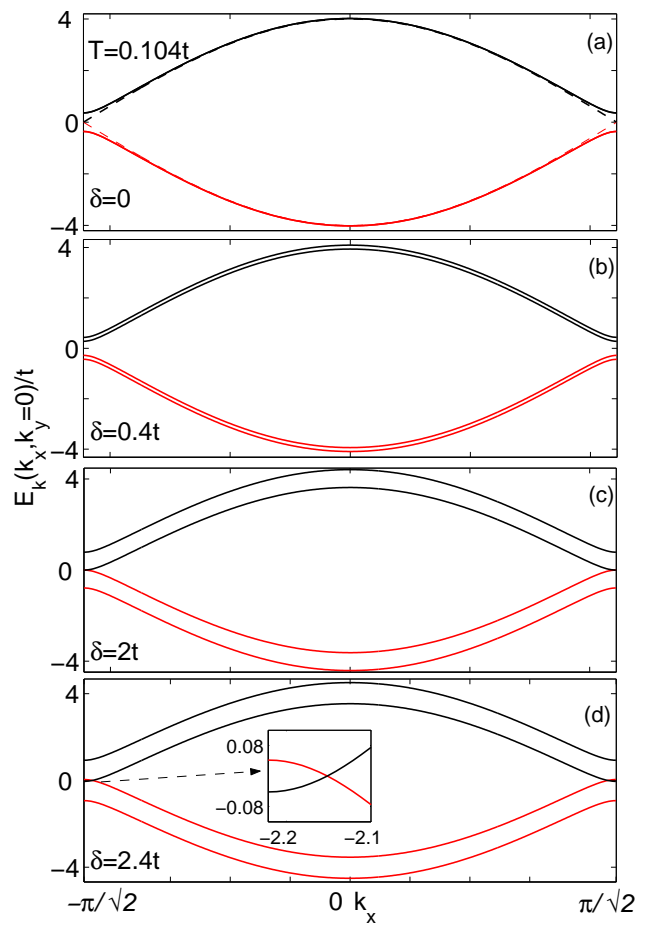


FIG. 6: The quasiparticle energy (in units of t) in momentum space along k_x (on x-axis), with $k_y = 0$ for average coupling $\bar{g} = t$ and various values of inhomogeneity $\delta = g^a - g^b$. (a) Spectrum when $g^A = g^B$. Dashed curve represents normal state $g^A = g^B = 0$ for reference. (b) Spectrum for $\delta = 0.4t$ (c) Spectrum for $\delta = 2t$, at transition to gapless state. (d) Spectrum for $\delta = 2.4t$, in gapless state. All spectra are shown at temperature $T = 0.104t$.

sence of coupling on these sites. These differences are illustrated in Fig. 5(a) and (b). It is also interesting to study the dependence of the subdominant condensate on inhomogeneity. The point where one of the coupling constants changes sign is clearly a singular point of the theory, such that at $T = 0$ this condensate is immediately depleted as soon as the subdominant coupling (B sublattice) becomes negative. We now discuss the reasons for this abrupt change in behavior.

C. Dispersion and density of states

In Eqs. (8), we have given the quasiparticle eigenenergies for this simple model; we now plot them in Fig. 6 along k_x for various representative cases. Of course the full quasiparticle spectrum retains the fourfold symmetry

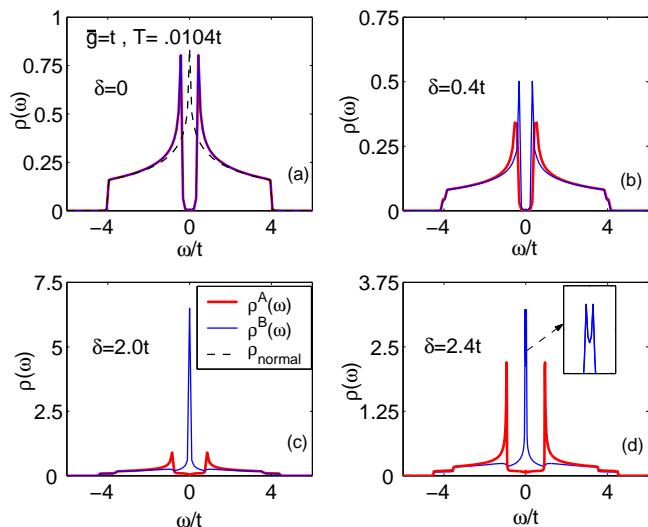


FIG. 7: Local density of states (LDOS) at sites A (red) and B (blue). (a) LDOS in homogeneous case, $\delta = 0$; (b) $\delta = 0.4t$, $\bar{g} = t$; (c) $\delta = 2t$, $\bar{g} = t$; (d) $\delta = 2.4t$, $\bar{g} = t$. The dashed line represents the normal state 2D tight binding band.

of the underlying lattice. Panel a) shows the dispersion in both the normal and homogeneous BCS case, respectively. Adding a small inhomogeneity with two attractive couplings leads to a splitting of these states, into four distinct eigenenergies (panel (b)), thereby reducing the overall spectral gap in the system. When one of the couplings passes through zero, a level crossing occurs at zero energy at the zone face (panel (c)). It is this level crossing which is responsible for the singular behavior in some observable quantities as one of the couplings becomes repulsive. It is accompanied by a filling of the gap by the states near the zone face. When the two couplings g_A and g_B have opposite signs, the eigenvalues change sign over the Brillouin zone. For example, in panel (d) of Fig. 6, E_2 is always positive, but E_1 is positive except in a narrow range $-\sqrt{\Delta^A |\Delta^B|} \leq \xi \leq \sqrt{\Delta^A |\Delta^B|}$.

Gapless behavior in s -wave superconductors with magnetic impurities¹⁴ can be associated with individual low-energy quasiparticle resonances, which arise near each magnetic impurity and then overlap to form an impurity band. The band appears as a residual density of states for sufficiently high impurity concentration. Similarly, the gapless superconductivity arising due to microscopically inhomogeneous sign-changing order parameters, which is found in the present paper, is reminiscent of respective low-energy Andreev states around so-called off-diagonal or phase impurities^{11,12}. One might imagine an ordinary s -wave superconductor into which a dilute lattice of phase impurities is introduced. As the lattice constant of such bound states is decreased, the bound state wave functions will interfere and the bound state energies will split, leading to a kind of gapless superconductivity related to that we find here for the dense case.

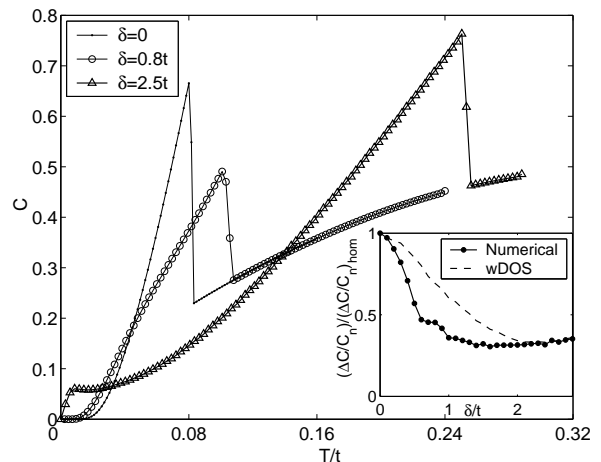


FIG. 8: Specific heat $C(T)/T$ of inhomogeneous system vs. $T/(4t)$. Solid line: BCS homogeneous superconductor with 2D tight-binding band. Circles: weak homogeneity $\delta = 0.8t$. Triangles: strong homogeneity $\delta = 2.5t$. Average coupling fixed to $\bar{g} = t$.

To observe this directly and trace the spectral features back to their respective sublattices, we construct the local density of states on A and B sites,

$$\rho^\alpha(\omega) = \sum_{n,\mathbf{k}} [|u_n^\alpha|^2 \delta(\omega - E_n) + |v_i^\alpha|^2 \delta(\omega + E_n)]. \quad (23)$$

Fig. 7 exhibits the LDOS on the two sublattices. In panels (a) and (b), when both couplings are positive, we clearly see a full spectral gap. But when one of the couplings tends to zero, as in (c), a sharp peak develops at the Fermi level on the associated sublattice. The system remains gapless as the coupling constant on this sublattice is made negative, as in (d). It should be noted, however, that the subgap states are not located at zero energy, as seen in Fig. 6d, where the dispersion is seen to flatten at the zone edge away from zero. This is reflected in a narrowly split resonance in the LDOS, as seen in Fig. 7.

D. Specific heat

To exhibit the consequences of the sublattice pairing inhomogeneity for thermodynamics, we calculate the specific heat from the temperature derivative of the entropy,

$$C = T \frac{dS}{dT}. \quad (24)$$

Here S for the free quasiparticles is given by

$$S = \sum_{\bar{k}, n=1,2} (f_n \log(f_n) + (1 - f_n) \log(1 - f_n)), \quad (25)$$

where $f_n \equiv f(E_n(\mathbf{k}))$, and the sum runs only over positive eigenvalues. In Figure 8, we plot these results for

a few examples. For a superconductor with a small amount of inhomogeneity—again keeping the average coupling fixed—it is clear that the critical temperature increases relative to the BCS case, the low- T temperature dependence remains exponential. On the other hand, when one of the coupling constants goes negative, the figure shows the existence of the residual density of states via a linear term in the specific heat at the lowest temperatures.

It is clear that the fractional jump in the specific heat, reflecting the condensation energy, decreases with increasing inhomogeneity, and is approximately constant for the gapless regime. Note that this ratio for the homogeneous case is not the conventional BCS value of 1.43, due to the non-parabolic band used here.

IV. SUPERFLUID DENSITY

As Aryanpour et al. have emphasized⁶, models of inhomogeneous pairing can lead to a variety of ground states, including insulating ones. To show that the states we discuss here are indeed superconducting, we use the criteria developed by Zhang et. al.¹³ for lattice systems. We calculate the superfluid density n_s , which is the sum of the diamagnetic response of the system (kinetic energy density) and paramagnetic response (current-current correlation function)

$$n_s/m = \langle -k_x \rangle - \Lambda(\omega = 0, \mathbf{q} \rightarrow 0). \quad (26)$$

The current-current response is defined as

$$\Lambda_{xx}(\bar{q}, i\omega_m) = \int_0^\beta d\tau e^{i\omega_m \tau} \langle j_x^P(\bar{q}, \tau) j_x^P(-\bar{q}, 0) \rangle \quad (27)$$

where the current at i^{th} site is given by

$$j_x^P(i) = it \sum_{\sigma} \left(c_{i+x,\sigma}^\dagger c_{i,\sigma} - c_{i,\sigma}^\dagger c_{i+x,\sigma} \right). \quad (28)$$

After evaluating the expectation value using the Bogoliubov operators in (7), we find the following relatively simple expression for the analytic continuation of the static homogeneous response:

$$\Lambda_{xx}(\omega = 0, \mathbf{q} \rightarrow 0) = 2 \sum_{\mathbf{k}} \left[4t \sin\left(\frac{k_x}{\sqrt{2}}\right) \cos\left(\frac{k_y}{\sqrt{2}}\right) \right]^2 \times \left(\frac{f(E_1) - f(E_2)}{E_1 - E_2} \right) \quad (29)$$

If the $E_i(\mathbf{k})$ do not change sign over the Brillouin zone, as is the case for the gapped phase $g_A, g_B > 0$, it is clear that this expression vanishes as $T \rightarrow 0$ as in the clean BCS case. This is no longer the case in the gapless regime $g_B \leq 0$, where a finite value of Λ , corresponding to a residual density of quasiparticles, is found at zero temperature.

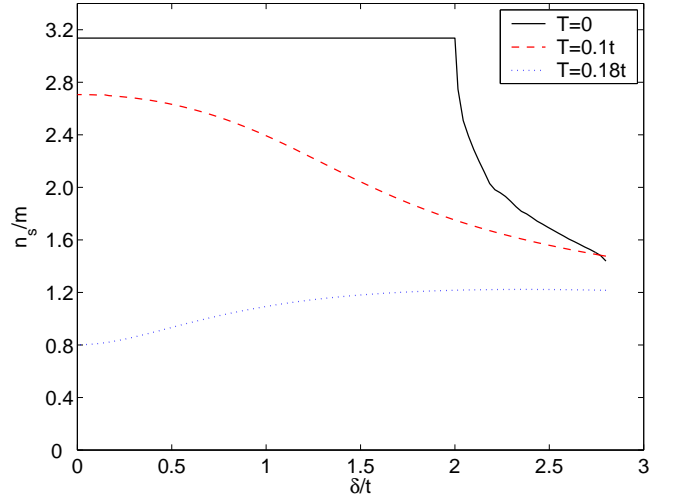


FIG. 9: Superfluid density n_s vs. inhomogeneity δ with fixed average coupling $\bar{g} = t$ at different temperatures $T = 0$ (solid) $0.1t$ (dashed), and $0.18t$ (dotted line). The range of inhomogeneities $2 \leq \delta/t$ corresponds to gapless superconductivity.

The other term we need to evaluate is the expectation value of the lattice kinetic energy density operator, which in the homogeneous BCS case is directly proportional to the superfluid weight $n_s/m = \langle -k_x \rangle$ at $T = 0$. The kinetic energy operator is defined as,

$$k_x(i) = -t \sum_{\sigma} \left(c_{i+x,\sigma}^\dagger c_{i,\sigma} + c_{i,\sigma}^\dagger c_{i+x,\sigma} \right) \quad (30)$$

In Fourier space, it can be written as:

$$k_x(i) = -t \sum_{\bar{k}_1, \bar{k}_2, \sigma} \left(c_{\bar{k}_1}^{A\dagger} c_{\bar{k}_2}^B e^{i(\bar{k}_2 - \bar{k}_1) \cdot \bar{r}_i} \left[2 \cos\left(\frac{k_{2y}}{\sqrt{2}}\right) e^{i\frac{k_{2x}}{\sqrt{2}}} \right] + h.c. \right) \quad (31)$$

After performing the canonical transformation and taking the expectation values we find

$$\langle k_x(i) \rangle = -2t \sum_{\mathbf{k}} \cos\left(\frac{k_y}{\sqrt{2}}\right) \times \sum_n \left\{ \left[u_n^{A*} u_n^B e^{i\frac{k_x}{\sqrt{2}}} + u_n^A u_n^{B*} e^{-i\frac{k_x}{\sqrt{2}}} \right] f(E_n) + \left[v_n^A v_n^{B*} e^{i\frac{k_x}{\sqrt{2}}} + v_n^{A*} v_n^B e^{-i\frac{k_x}{\sqrt{2}}} \right] (1 - f(E_n)) \right\} \quad (32)$$

which is, remarkably, the same for sites A or B, corresponding to the uniform proximity-induced condensate amplitude found in section III B. In terms of the eigenvectors and eigenvalues given by Eqs. (9), (10), (11) and (12), we can write

$$\langle k_x(i) \rangle = 2 \sum_{\bar{k}} \xi_{\bar{k}} \frac{x_1 x_2}{x_1^2 + x_2^2} \left[\tanh\left(\frac{\beta E_1}{2}\right) + \tanh\left(\frac{\beta E_2}{2}\right) \right] \quad (33)$$

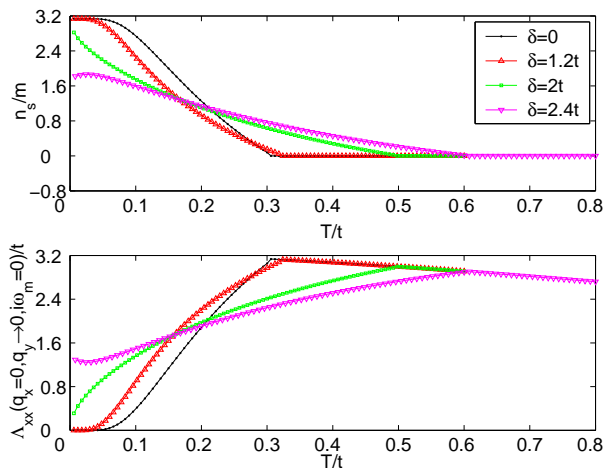


FIG. 10: The upper graph shows the superfluid density n_s as a function of temperature for various inhomogeneity parameters $\delta/t = 0$ (black), 1.2 (red), 2 (green) and $\bar{g} = t$ (magenta). The lower panel shows the current current correlation $\Lambda_{xx}(T)$.

For the case when $g^A, g^B > 0$ at $T = 0$, we can simplify this expression as

$$\langle -k_x(i) \rangle = 2 \sum_{\bar{k}} 2 \frac{\xi_{\mathbf{k}}^2}{\sqrt{(\Delta_0^A + \Delta_0^B)^2 + 4\xi_{\mathbf{k}}^2}}, \quad (34)$$

which is manifestly positive; hence, the system is a superconductor and displays a conventional Meissner effect at $T = 0$. The expression also shows explicitly that the superfluid density on each site corresponds to the average superconducting order parameter over the system.

Fig. 9 show how the superfluid weight (n_s) changes as the inhomogeneity is increased. At $T = 0$, n_s for this model is a constant and equal to the value for the homogeneous system, whenever the system is fully gapped, since the average gap remains the same. In the same system, recall, the transition temperature increases monotonically with inhomogeneity. As one increases the inhomogeneity further with fixed average coupling, there is a critical value δ_c for which the system enters the gapless phase, at which the superfluid density drops abruptly. The temperature dependence of such a case is exhibited, along with others, in Fig. 10, and we see that this discontinuity corresponds to the creation of a finite residual normal fluid of uncondensed quasiparticles. Exactly at δ_c ($= 2t$ in Fig. 10), this behavior is marginal, but for any $\delta > 2t$ in the Figure, the residual normal fluid density $\Lambda_{xx}(T = 0)$ is nonzero.

If \bar{g} is held fixed and inhomogeneity δ increased further, there is no mean-field transition to the metallic state, as indicated e.g. by the dashed-dotted line in Fig. 1 which we have investigated in this paper. Instead, T_c increases monotonically while the superfluid density begins to fall at $T = 0$ when the system enters the gapless phase at δ_c . Eventually, the decrease in n_s must lead to large phase

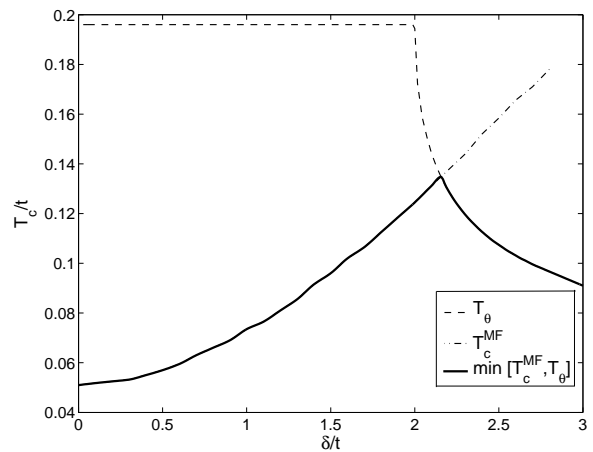


FIG. 11: Mean field critical temperature T_c (dashed-dotted line) and phase ordering temperature T_θ (dashed line) vs. inhomogeneity δ for fixed average interaction $\bar{g} = t$. The solid line is the minimum of the two curves at any δ .

fluctuations and the breakdown of the mean field theory described here. To estimate when this occurs, we follow Emery and Kivelson¹⁷ and define a characteristic phase ordering temperature

$$T_\theta = \hbar^2 n_s(0) \ell / 4m^*, \quad (35)$$

which will now decrease in the gapless phase, following the superfluid density. For quasi two-dimensional superconductors, the length scale ℓ is a larger of the average spacing between layers d or $\sqrt{\pi} \xi_\perp$, where ξ_\perp is the superconducting coherence length perpendicular to the layers. Although a determination of ℓ is beyond our simple model, it is qualitatively irrelevant in the presence of significant abrupt drop of the superfluid density. Taking simply $\ell \sim a$, which is within a factor of 2-3 of both d and $\sqrt{\pi} \xi_\perp$ in the cuprates, we may now obtain a crude measure of the *optimal inhomogeneity* needed to maximize the true ordering temperature in this model. In Fig. 11, we now plot both the mean field T_c and the putative phase ordering temperature as a function of inhomogeneity δ . We see that the two curves cross very close to the phase boundary δ_c (at $\delta = 2t$ in the Figure), due to the steep drop in n_s there. It therefore appears that the optimal inhomogeneity *within the current scheme* occurs for a checkerboard-like pairing interaction with attractive interaction on one sublattice and zero interaction on the other.

V. CONCLUSIONS

We have presented and solved a simple mean-field model of a superconductor with inhomogeneous pairing varying on an atomic scale. The model simply takes a different value for pairing on each of two interpenetrating

sublattices. The inhomogeneity can be increased while keeping the average pairing in the system fixed, thus allowing the effect of inhomogeneity on various properties to be discussed. Many results for this model were presented in analytic form. As pointed out by earlier workers, we find that increasing pairing inhomogeneity enhances T_c . We have presented analytical results reflecting this effect, and calculated the spectrum and thermodynamic properties as well. The enhancement of T_c is accompanied by a closing of the spectral gap and eventually by the appearance of gapless phase in the quasiparticle spectrum of the “s-wave” superconductor. While these results have been obtained at the mean field level, because the length scale of the variation of the pairing interaction is so short we do not expect fluctuations to change them significantly³, at least until the superfluid density is substantially suppressed.

The last caveat does not seem to be particularly restrictive, however. The enhanced T_c found in the inhomogeneously paired system is accompanied by a reduction in condensation energy, but the system maintains a constant $T = 0$ superfluid density until a critical value of the

inhomogeneity, when a level crossing of two quasiparticle energies forces the system into the gapless phase. Until this point, the condensate at $T = 0$ is spatially homogeneous for any value of the interaction inhomogeneity, even when the interaction on a given sublattice is zero; this reflects the strong proximity coupling between the sublattices. As inhomogeneity increases further, we have argued that the decrease in the superfluid density leads fairly rapidly to a decrease in the phase ordering temperature; we find, therefore, that the optimal inhomogeneity is reached close to the checkerboard pattern of interactions, with attractive pairing on one sublattice and zero on the other.

Our results suggest that in superconducting systems with short coherence length, a modulated pairing interaction at the atomic scale may provide a route to high temperature superconductivity.

The authors are grateful for useful conversations with S. A. Kivelson. Research was partially supported by DOE DE-FG02-05ER46236 (PJH and VM) and RFBR grant 08-02-00842 (YSB).

* Electronic address: vivekm@phys.ufl.edu

† Electronic address: pjh@phys.ufl.edu

¹ Oystein Fischer, Martin Kugler, Ivan Maggio-Aprile, Christophe Berthod, and Christoph Renner, *Rev. Mod. Phys.* **79**, 353 (2007).

² J.M. Tranquada, in *Handbook of High-Temperature Superconductivity*, J.R. Schrieffer and J.S. Brooks, editors, Berlin, Springer-Verlag, 2007.

³ I. Martin, D. Podolsky and S. A. Kivelson, *Phys. Rev. B* **72**, 060502 (2005); E. Arrigoni and S. A. Kivelson, *Phys. Rev. B* **68**, 180503 (2003).

⁴ G. Alvarez, M. Mayr, A. Moreo, and E. Dagotto, *Phys. Rev. B* **71**, 014514 (2005).

⁵ Y. L. Loh and E. W. Carlson, *Phys. Rev. B* **75**, 132506 (2007).

⁶ K. Aryanpour, E. R. Dagotto, M. Mayr, T. Paiva, W. E. Pickett and R. T. Scalettar, *Phys. Rev. B*, **73**, 104518 (2006); K. Aryanpour, T. Paiva, W. E. Pickett and R. T.

Scalettar, *Phys. Rev. B* **76**, 184521 (2007).

⁷ Yu. S. Barash, P. I. Nagornykh, *JETP Lett.* **83**, 376 (2006).

⁸ W.-F. Tsai, H. Yao, A. Läuschli and S.A. Kivelson, arXiv:0803.0933 (2008).

⁹ T.S. Nunner, B.M. Andersen, A. Melikyan and P.J. Hirschfeld, *Phys. Rev. Lett.* **95**, 177003 (2005).

¹⁰ A. Montorsi, D. K. Campbell, *Phys. Rev.* **53**, 5153 (1996).

¹¹ A.K. Chattopadhyay, R.A. Klemm and D. Sa, *J. Phys. Cond. Matt.* **14**, L577 (2002).

¹² B.M. Andersen, A. Melikyan, T.S. Nunner, and P.J. Hirschfeld, *Phys. Rev. Lett.* **96**, 097004 (2006).

¹³ D. J. Scalapino, S. R. White and S. Zhang, *Phys. Rev. B* **47** (1993).

¹⁴ A. A. Abrikosov, L. P. Gor’kov, *JETP* **12**, 1243 (1961).

¹⁵ H. Shiba, *Prog. Theor. Phys.* **40**, 435 (1968).

¹⁶ A. I. Rusinov, *JETP Lett.* **9** 85 (1969).

¹⁷ V. J. Emery, S. A. Kivelson, *Nature* **374**, 434 (1995).